Cell Reports, Volume *42*

Supplemental information

Multi-omics comparison of malignant and normal uveal melanocytes reveals molecular features of uveal melanoma

David Gentien, Elnaz Saberi-Ansari, Nicolas Servant, Ariane Jolly, Pierre de la Grange, Fariba Némati, Géraldine Liot, Simon Saule, Aurélie Teissandier, Deborah Bourc'his, Elodie Girard, Jennifer Wong, Julien Masliah-Planchon, Erkan Narmanli, Yuanlong Liu, Emma Torun, Rebecca Goulancourt, Manuel Rodrigues, Laure Villoing Gaudé, Cécile Reyes, Matéo Bazire, Thomas Chenegros, Emilie Henry, Audrey Rapinat, Mylene Bohec, Sylvain Baulande, Radhia M'kacher, Eric Jeandidier, André Nicolas, Giovanni Ciriello, Raphael Margueron, Didier Decaudin, Nathalie Cassoux, Sophie Piperno-Neumann, Marc-Henri Stern, Johan Harmen Gibcus, Job Dekker, Edith Heard, Sergio Roman-Roman, and Joshua J. Waterfall

Supplementary Figure 1: MP41 and MP46 genomic and transcriptomic features, related to Figure 2.

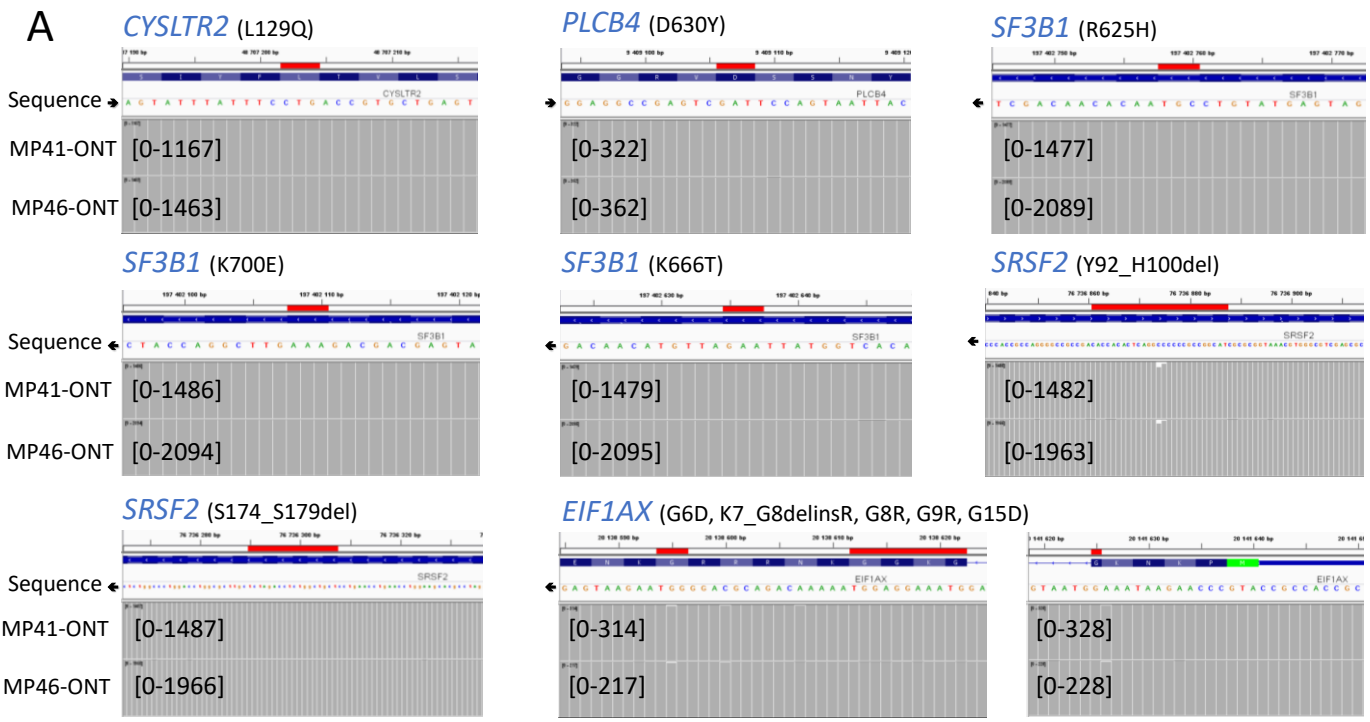

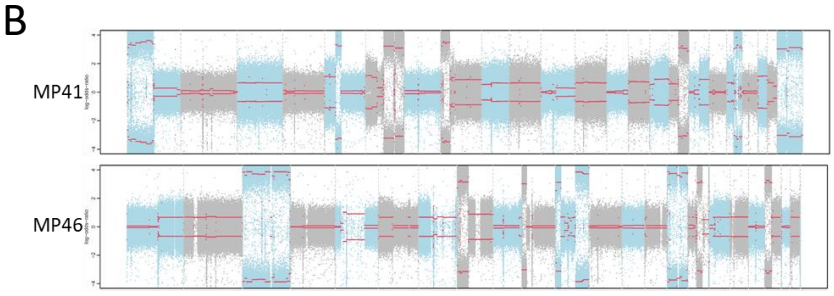

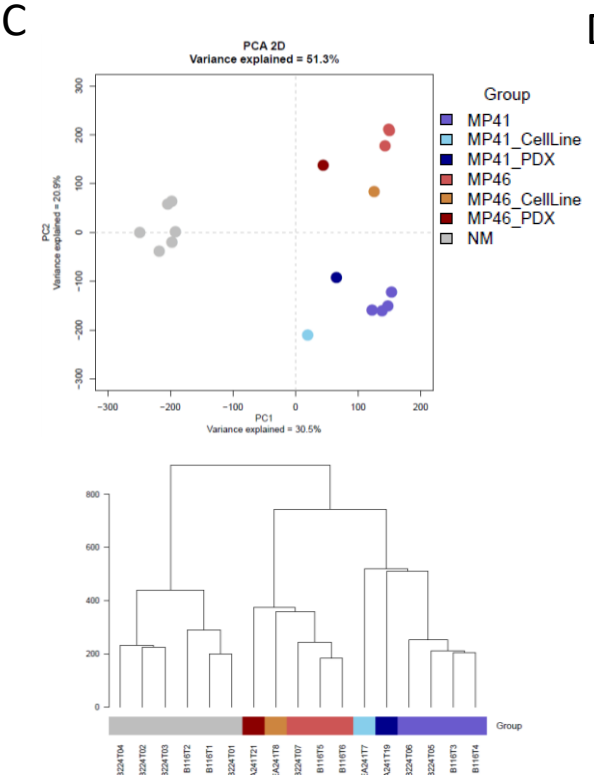

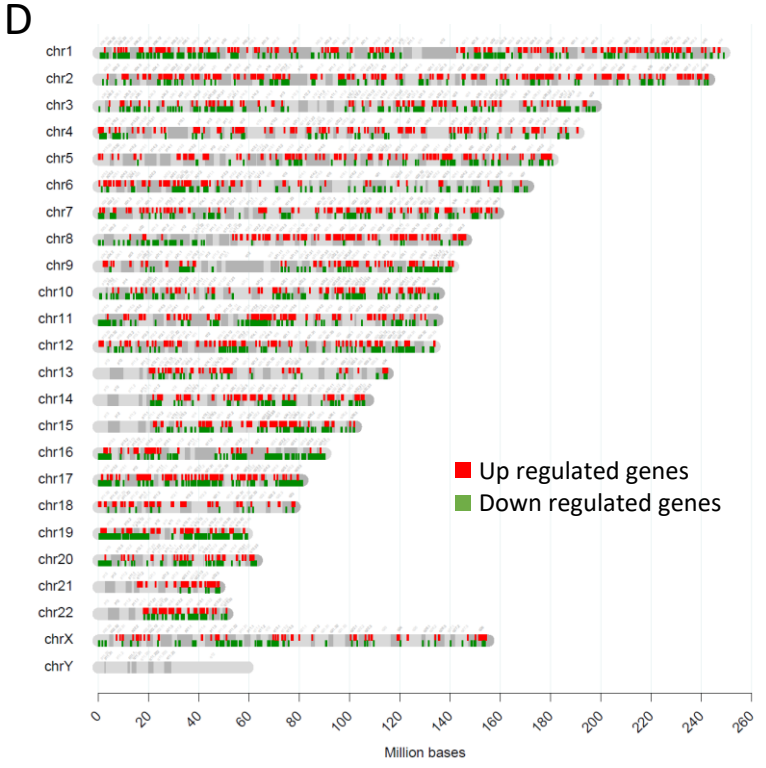

Supplementary Figure 1: MP41 and MP46 genomic and transcriptomic features, related to Figure 2. A) IGV analysis of targeted ONT sequencing of *CYSLTR2*, *PLCB4*, *SF3B1, SRSF2* , *EIF1AX* genes. Known hotspot or main mutation locus in parentheses are highlighted in red on the genomic bar. Mutations are named according to amino acid mutations. Values in brackets correspond to the scale of depth coverage in a considered window. B) Allele frequency facets CNV profile of MP41 and MP46 calculated from WGS dataset. C) Comparison of the transcriptomes of sorted cells from MP41 and MP46 PDX , MP41 and MP46 cell lines grown in cell culture, and normal melanocytes grown in cell culture via principal component analysis (top) and unsupervised hierarchical clustering (bottom). D. Genomic localization of the 2334 upregulated genes and the 3066 down regulated genes are represented respectively in red and green on a chromosome view

Supplementary Figure 2: Main regulated pathways from the regulated genes shared in MP41 and MP46 vs NM, related to Figure 2.

A. Cell cycle (HSA04110, KEGG)

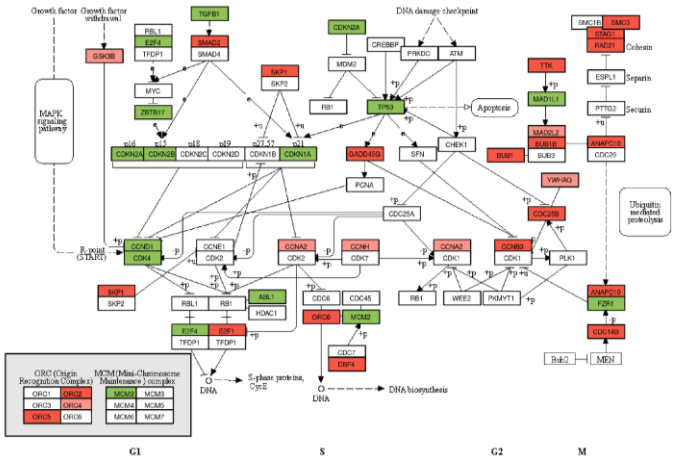

B. Homologous recombination (HSA03440, KEGG)

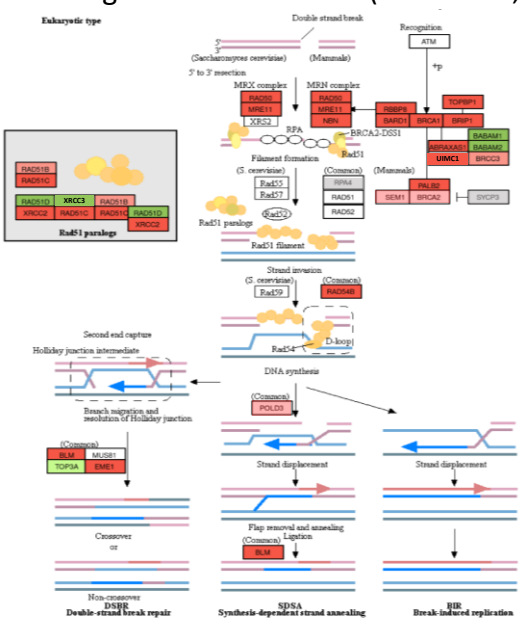

C. Fanconi Anemia (HSA03460, KEGG)

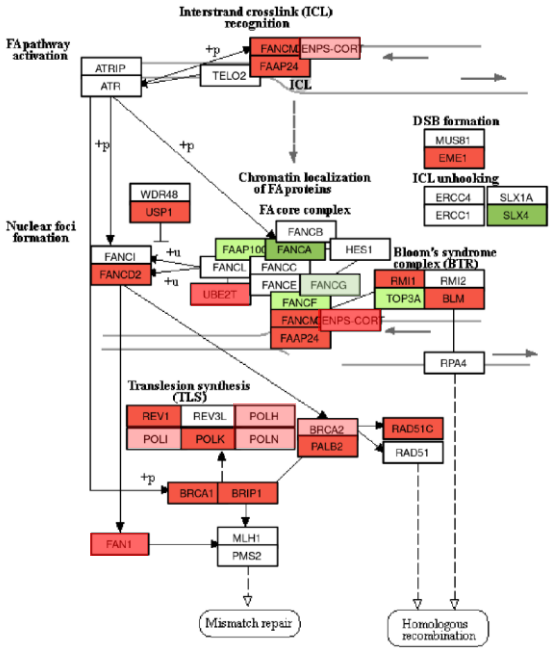

D. Non-Homologous End-Joining (HSA 03450, KEGG)

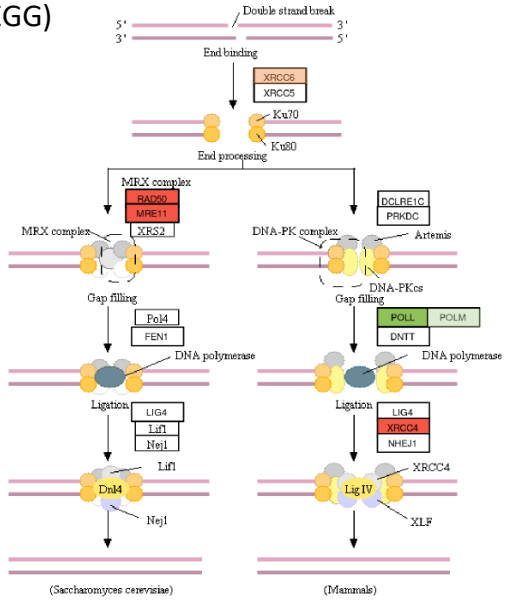

E. p53 signaling pathway (HSA04115, KEGG)

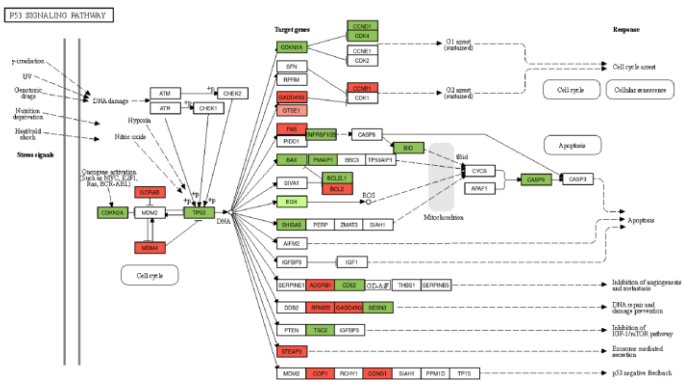

F. Apoptosis pathway (HSA04210, KEGG)

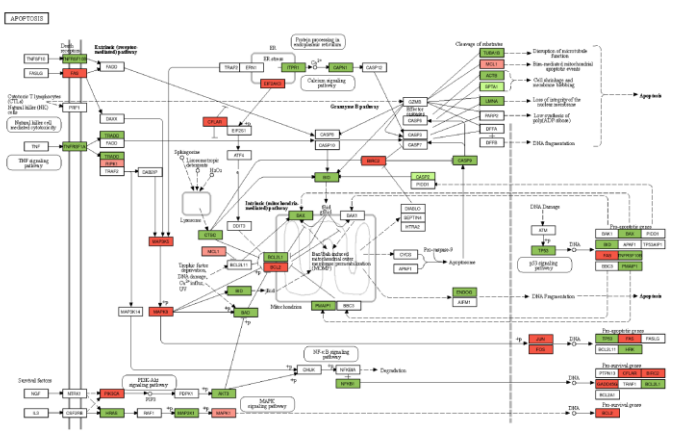

Supplementary Figure 2: Main regulated pathways from the regulated genes shared in MP41 and MP46 vs NM, related to Figure 2. Gene names are colored depending on their regulation: non-regulated genes are in white boxes, upregulated genes in red boxes and downregulated genes in green boxes. Light colors indicate a significant regulation in MP41 vs NM or in MP46 vs NM, and dark colors indicate a significant regulation observed in both comparisons. A) Cell cycle pathway (HSA04110, KEGG): 43 regulated genes out of 124 genes in pathway (min p-value: $5.30x10^{-07}$, 28 Up & 15 Down). B) Homologous recombination (HR) pathway (HSA03440, KEGG): 21 regulated genes out of 41 genes in pathway (min p-value: $5.99x10^{-09}$, 17 Up & 4 Down). C) Fanconi Anemia pathway (FA, HSA03460, KEGG): 19 regulated genes out of 54 genes in pathway (min p-value: $2.94x10^{-4}$, 13 Up & 6 Down). D) Non-homologous end joining pathway (NHEJ, HAS03450, KEGG): 4 regulated genes out of 13 genes in the pathway (min p-value: $8.22x10^{-2}$, 3 Up & 1 Down). E) P53 signaling pathway (HSA04115, KEGG): 32 regulated genes out of 72 genes in the pathway (min p-value: $1.18x10^{-6}$, 14 Up & 18 Down). F) Apoptosis pathway (HSA04115, KEGG): 52 regulated genes out of 136 genes in the apoptosis pathway (min p-value: $2.47x10^{-07}$, 20 Up & 32 Down).

Supplementary Figure 3: Telomere and FISH analysis, related to Figure 3.

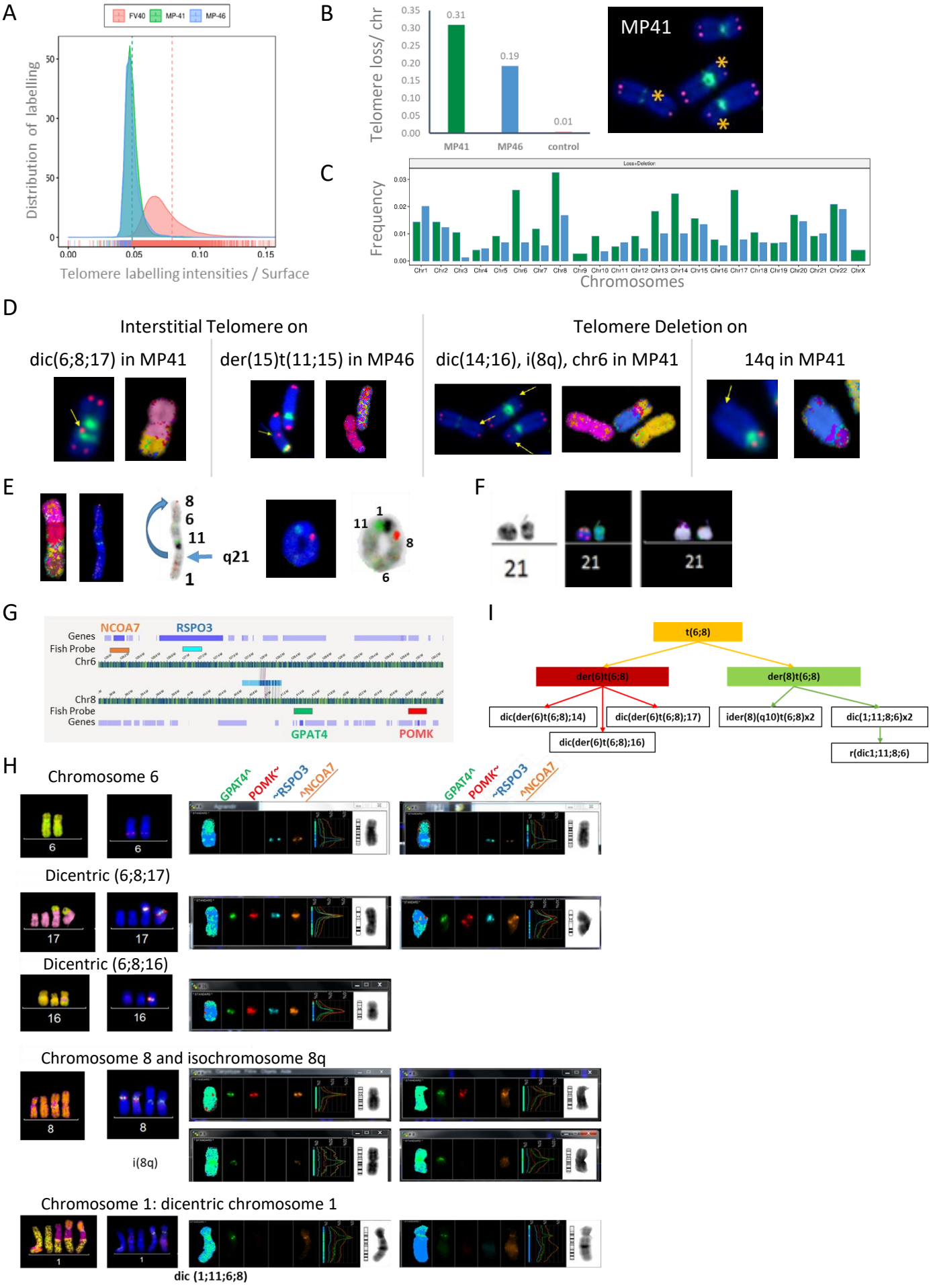

Supplementary Figure 3: Telomere and FISH analysis, related to Figure 3. A) Telomere fluorescence intensities of the 3 models as function of cell area. B) Rate of telomere loss per chromosome in MP41, MP46 compared to controls. Yellow stars highlight telomere loss on 3 chromosomes of MP41. C) Frequency of telomere loss and deletion per chromosome in MP41 and MP46. D) Example of telomere defects as interstitial telomere observed on dicentric (6;8;17) in MP41, and on a derivative chr15. Telomere deletion on dic(14;16) , i8q, and chr6, and chr 14q are illustrated. E) A dic(1)t(1;11;6;8) and a ring chromosome probably coming from a breakpoint on 1q21 leading to a ring chromosome (r(dic(1;11;6;8)). F) A ring chromosome in MP46 (r(21)). G) Specific probes (Empire Genomic, USA) designed for the detection of 4 genes: *NCOA7* (orange), *RSPO3* (blue), *GPAT4* (green), and *POMK* (red). FISH probes are represented on the optical map showing the t(6;8) generated from the Bionano analysis in MP41. H) The presence of *RSPO3* and *NCOA7* is detected in chromosome 6 without rearrangements . A dic(6;8;17) and a dic(6;8;16) are showing the presence of *GPAT4* and *POMK* genes in addition to *RSPO3* and NCOA7 in the breakpoint of the aberration. The i(8q) shows the presence of *GPAT4* and *NCOA7*, as the dic(1;11;6;8) harboring an insertion of the *GPAT4* and *NCOA7* in the breakpoint of this rearrangement. I) Possible mechanisms in the formation of these rearrangements implicated chromosome 6 and 8.

Supplementary Figure 4: DNA optical mapping and multispectral FISH highlight chromosome aberrations and DNA rearrangements in UM models, related to Figure 3.

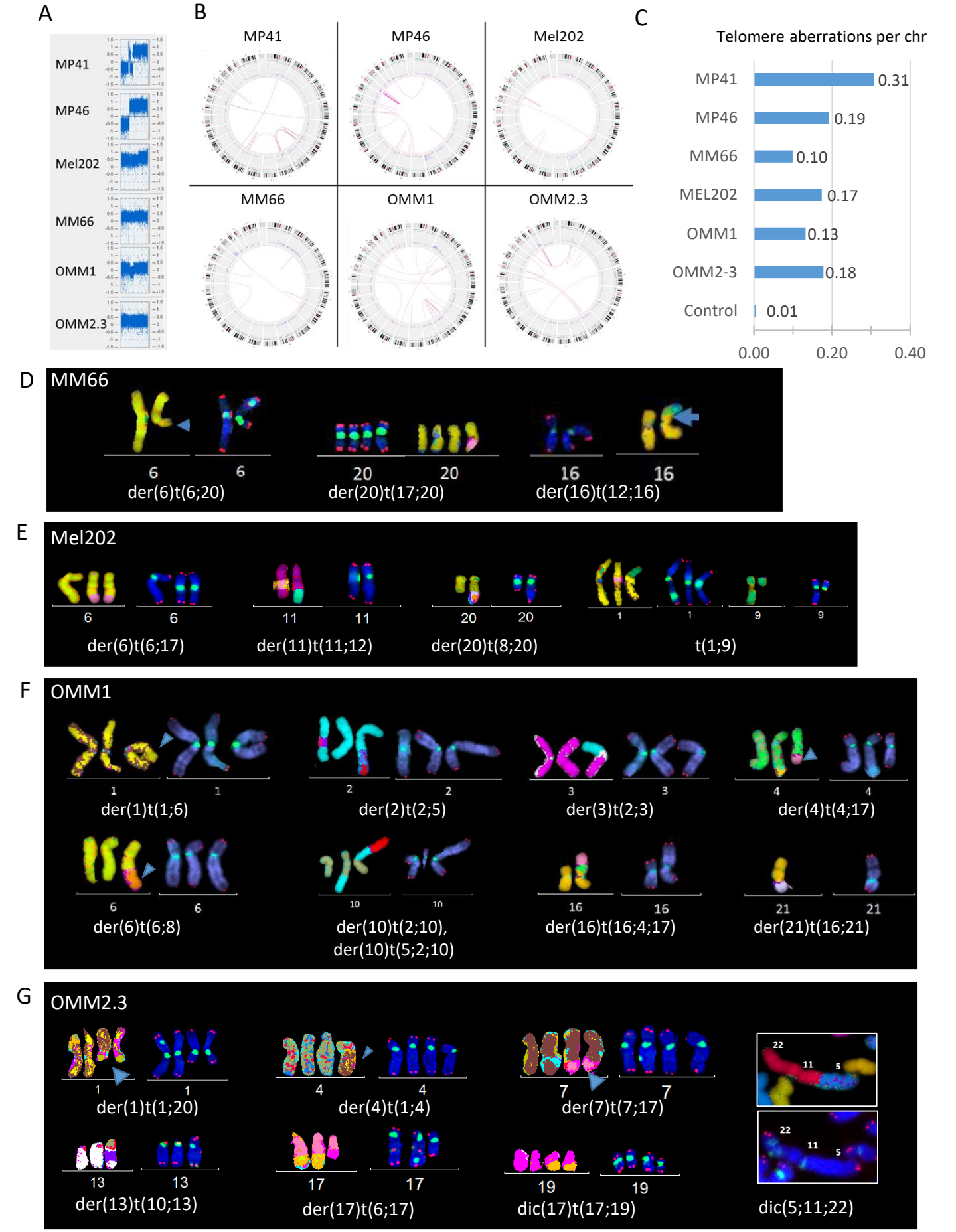

Supplementary Figure 4: DNA optical mapping and multispectral FISH highlight chromosome aberrations and DNA rearrangements in UM models, related to Figure 3. A) Log2 ratio generated from Cytoscan HD microarrays of chr8 in UM models. B) Circos plot generated from DNA optical mapping illustrate main SVs as translocations. C) Telomere aberrations per chromosome on UM cell models as MP41, MP46, MM66, Mel202, OMM1, OMM2.3 and normal fibroblasts as controls. Main derivative and dicentric chromosomes of D) MM66, E) Mel202, F) OMM1, G) OMM2.3. FISH and TC pictures of derivative and dicentric chromosomes are presented. Blue triangles point small parts of a donor chromosome.

Supplementary Figure 5: Identification of BAP1 deletion leading to BAP1 loss of expression, related to Figure 4.

A. *BAP1* gene expression

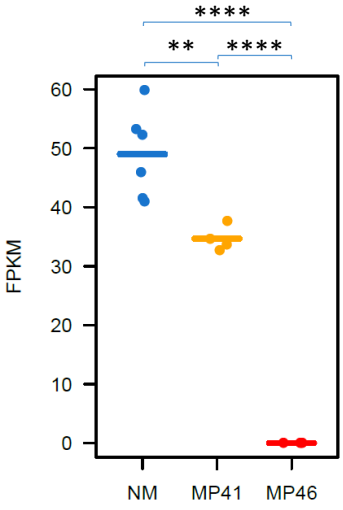

B. *PHF7* gene expression

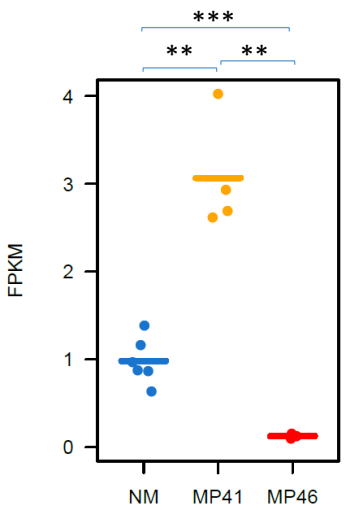

C. *BAP1* amplicon sequencing

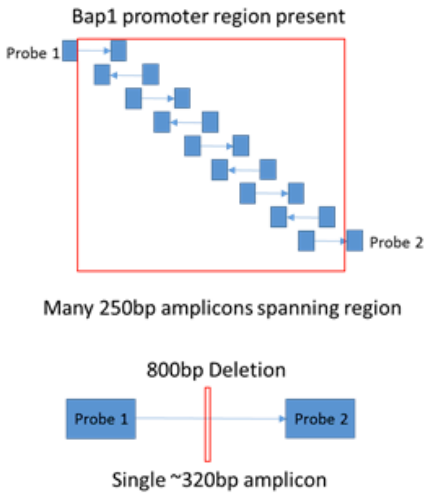

D.

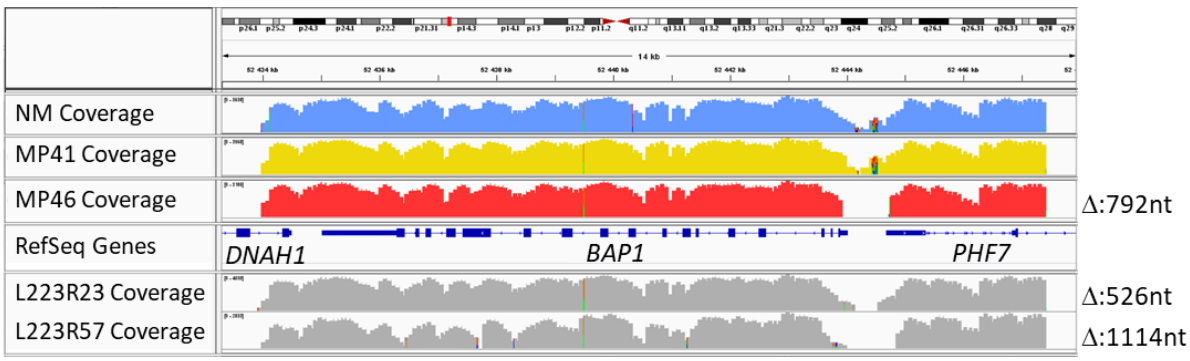

E. BAP1 IHC (40X)

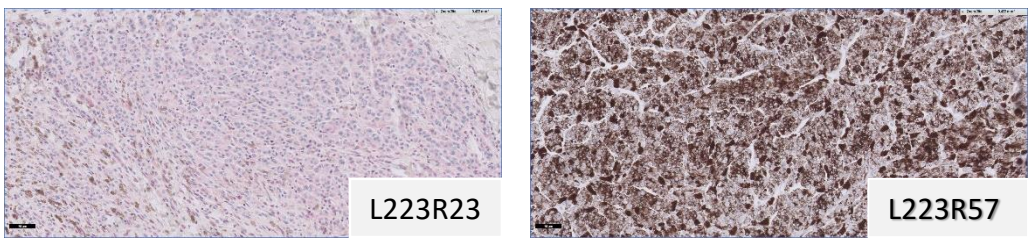

F.

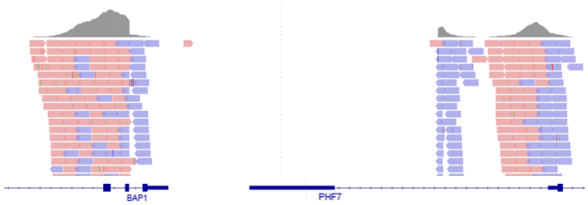

G. BAP1 IHC

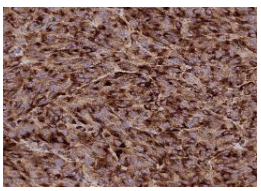

H.

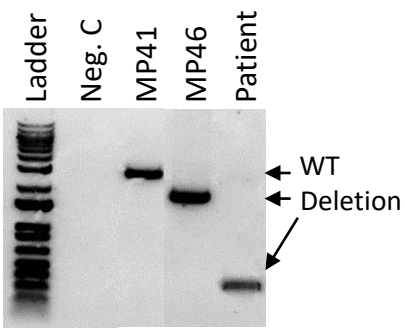

Supplementary Figure 5: Identification of BAP1 deletion leading to BAP1 loss of expression, related to Figure 4. Gene expression detection based on RNAseq analysis (FPKM counts) of A) *BAP1* and B) *PHF7* in NM, MP41 and MP46 samples. C) Targeted sequencing based on tilling amplicons (250bp) to characterize *BAP1* mutations in a series of 53 UM recently grafted for new UM PDX at Institut Curie. D) Detection of *BAP1/PHF7* promoter deletion in IGV. Blue track corresponds to NM sample, yellow track corresponds to MP41 and red track corresponds to MP46. Gray tracks correspond to new UM cases with a low coverage on *BAP1* promoter associated to a loss of BAP1 protein expression assessed by IHC (E). Example of *BAP1* 5'UTR/promoter deletion identified in clinical daily practice. F) Identification of BAP1 promoter deletion (2.2kb) based on exome analysis. G) Validation of the loss of BAP1 expression in nucleus by IHC. H) Confirmation of the deletion of *BAP1* promoter by long range PCR in MP46 and new patient's tumor.

Supplementary Figure 6: Normalization of Hi-C Data and comparison of compartment interaction scores per type of compartment, and interaction score distribution per copy number status and number of A/B compartments, related to Figure 5.

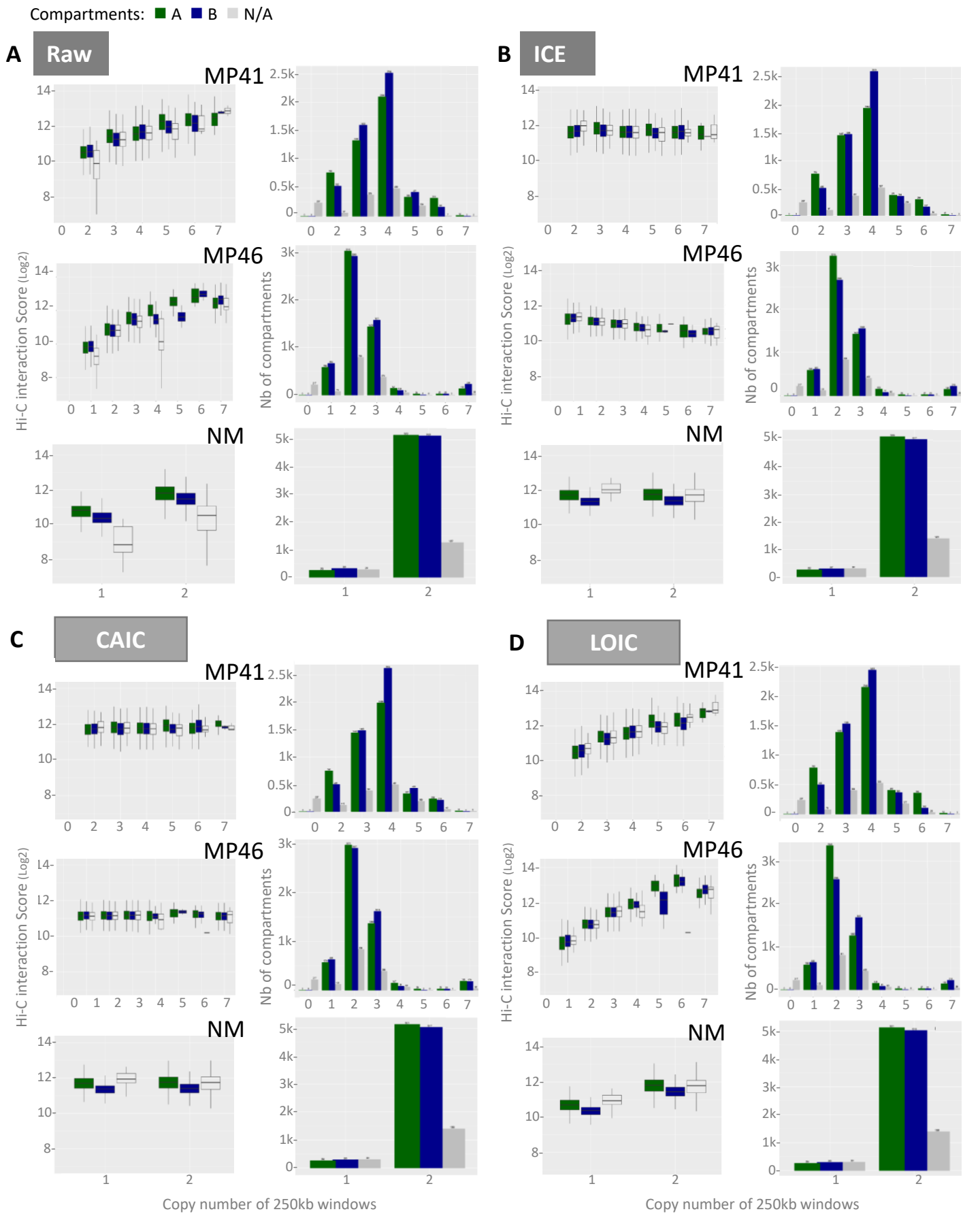

Supplementary Figure 6: Normalization of Hi-C Data and comparison of compartment interaction scores per type of compartment, and interaction score distribution per copy number status and number of A/B compartments, related to Figure 5. From each normalization method of Hi-C data generated for MP41, MP46 and NM, interactions scores for all compartments were separated on A/B status, and undefined status. Log2 Hi-C interaction scores are depicted across copy number status defined at 250kb window resolution. Interactions score from A) raw data, or after B) ICE, C) CAIC and D) LOIC normalization are compared for MP41, for MP46 and for NM. Per UM and NM panels, box plots and histograms show respectively compartment interaction scores and number of interactions. Green, blue and grey box plots and bars correspond respectively to euchromatin / A compartment, heterochromatin / B compartment, and not defined compartments

Supplementary Figure 7: *PRAME* locus transcription factors (TF) upregulated in UM models, related to Figure 6.

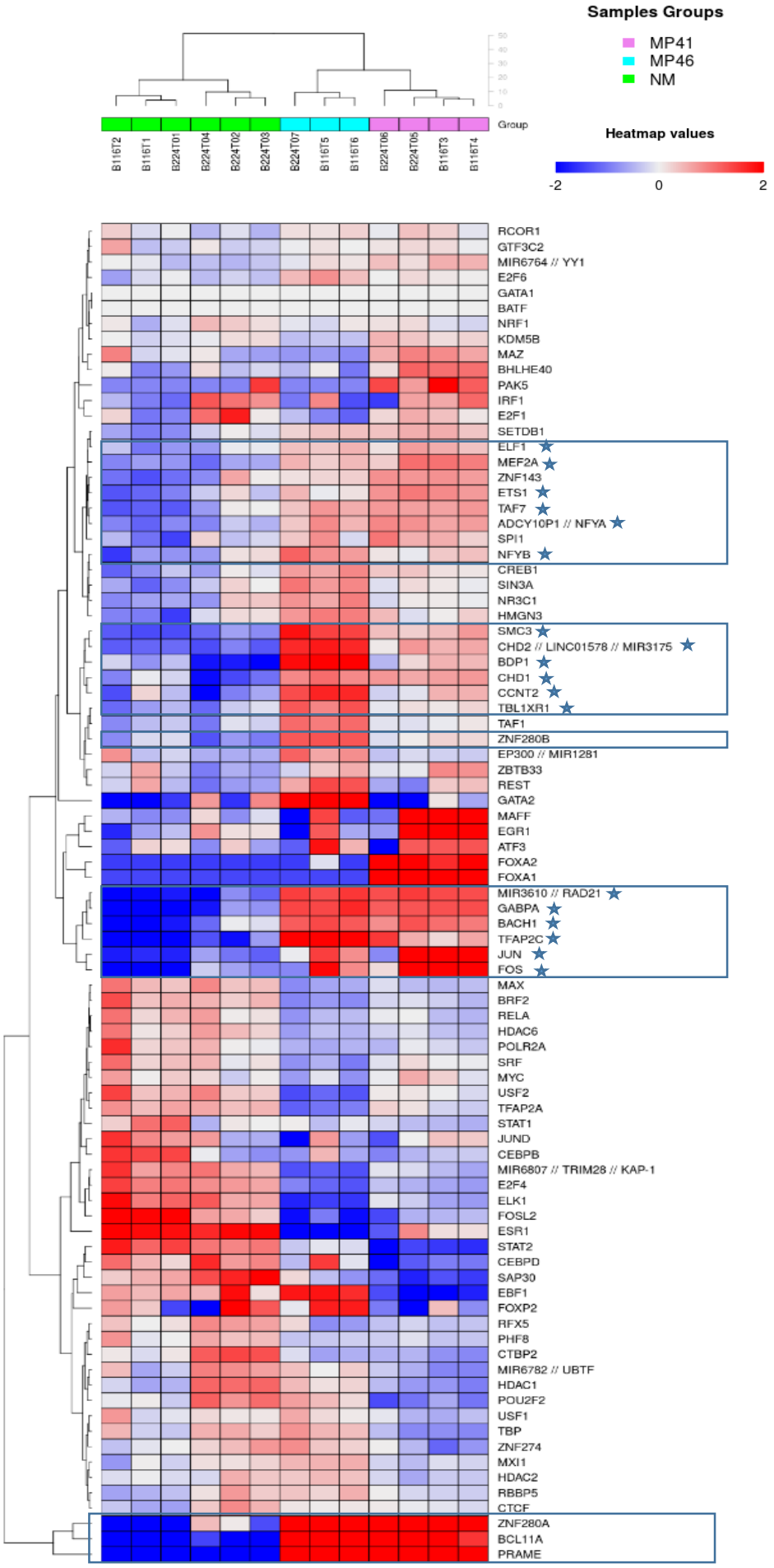

Supplementary Figure 7: PRAME locus transcription factors (TF) upregulated in UM models, related to Figure 6. Hierarchical clustering of TFs enriched at PRAME locus in ENCODE. Blue stars indicate TFs with significantly upregulated expression in MP41 and in MP46 vs NM

Supplementary Table 3: List of guide RNAs used for ONT sequencing, related to STAR Methods

Gene Symbol	Design ID	Comment	Strand	Sequence
CYSLTR2	CD.Cas9.YKJD7688.AC	CYSLTR2_start	+	GAATTGGTACGTCTTCTTAG
	CD.Cas9.VHHC4155.AG	CYSLTR2_end	-	CTGAGCCATGTAGTGTACTG
EIF1AX	CD.Cas9.JXHY8388.AH	EIF1AXstart	+	CTCTGCATCGTATAAAGTAA
	CD.Cas9.MCMB0850.AE	EIF1AXend	-	CTCCCACAACGCGTCTCCCT
PLCB4	CD.Cas9.YPRQ6246.AJ	PLCB4start	+	TGGTTTATCCTACAACAGTG
	CD.Cas9.VGXP9394.AA	PLCB4end	-	TTGGCAGAGAACCATTCACC
SF3B1	CD.Cas9.NMPG1247.AA	SF3B1start	+	GTAGCTATCTTCAAGTATAG
	CD.Cas9.JCGF6379.AE	SF3B1end	-	AGTGTTAATGACCAGCCATC
SRSF2	CD.Cas9.VTBZ3294.AE	SRSF2start	+	ATTATACCTACAACCTGTTC
	CD.Cas9.PYZX6456.AN	SRSF2end	-	AAGCACTCTTCAGACGGAGA

Supplementary Table 4: Somatic copy number alterations in UM models identified by WGS, related to Figure 2

Models	Losses (L: Loss, M: Monosomy)	Gains (G)
MP41	L1p, M3, L6q, L8p, L9, L10, L12q, L16q	G1q, G6p, G8q, G11q,G12p, G16p, G21
MP46	Isodisomy 3, L8p, L16q, L20p	G1q, G2,G6p, G7, G8q, G17, G18, G20q, G21, G22

Supplementary Table 6 : Number of genes by HiC compartment status, related to Figure 5

	AAA	AAB	ABA	ABB	BAA	BAB	BBA	BBB	No compartment	Multi-compartment	**Total**
Expressed in both / same regulation	**2590**	**286**	**212**	**96**	**63**	**84**	**144**	**360**	**1291**	**274**	**5400**
Expressed in both / different regulation	164	22	12	6	4	12	7	31	127	18	**403**
Expressed in both / regulated in one	2120	249	173	78	49	84	104	357	1252	190	**4656**
Expressed in both / regulated in none	**1231**	**170**	**87**	**51**	**52**	**57**	**79**	**202**	**822**	**96**	**2847**
Expressed in one / regulated in one	536	82	59	21	22	21	49	143	336	49	**1318**
Expressed in one / regulated in none	277	32	20	11	20	17	27	68	277	12	**761**
Expressed in none / regulated in none	**20368**	**3816**	**2564**	**1429**	**1416**	**2018**	**2780**	**10398**	**14190**	**451**	**59430**
Total	27286	4657	3127	1692	1626	2293	3190	11559	18295	1090	**74815**

Supplementary Table 7 : Random forest classification and probability to predict UM cell lines as NM or PDX based on histone mark localization patterns, related to Figure 6.

Cell line	Replicate ID	Histone Mark	Prediction	Probability
MP41	D1410C14	H3K27me3	MP41 PDX	0.647
MP41	D1410C20	H3K27me3	MP41 PDX	0.637
MP46	D1410C17	H3K27me3	MP46 PDX	0.646
MP46	D1410C23	H3K27me3	MP46 PDX	0.651
MP41	D1410C15	H3K4me3	MP41 PDX	0.599
MP41	D1410C21	H3K4me3	MP41 PDX	0.608
MP46	D1410C18	H3K4me3	MP46 PDX	0.56
MP46	D1410C24	H3K4me3	MP46 PDX	0.57
MP41	D1410C16	H2AUb	NM	0.508
MP41	D1410C22	H2AUb	MP41 PDX	0.669
MP46	D1410C19	H2AUb	MP46 PDX	0.612
MP46	D1410C25	H2AUb	MP46 PDX	0.604